Hydroxyl-Radical-Initiated Oxidation Mechanism of Bromopropane

Mónica Martínez-Avilés, Claudette M. Rosado-Reyes, and Joseph S. Francisco*

Department of Chemistry and Department of Earth and Atmospheric Sciences, Purdue University West Lafayette, Indiana 47907

Received: April 21, 2008; Revised Manuscript Received: June 12, 2008

Bromopropane has been considered as a replacement for chlorofluorocarbons used as the active component of industrial cleaning solvents, more specifically for HCFC-141b. The proposed mechanism for the atmospheric oxidation of bromopropane is studied via ab initio methodology. Ab initio molecular orbital methods at the CCSD(T)/6-311++G(2df,2p)//MP2/6-31G(d) level of theory have been used to determine the structure and energetics of the 58 species and transition states involved in the atmospheric oxidation of bromopropane. The calculations show that the major oxidation species is bromoacetone. Other brominated species that result from the oxidation are $BrCH_2CH_2C(O)H$, $BrC(O)CH_2CH_3$, and BrC(O)H, potential new bromine reservoir species that result from bromopropane in the atmosphere.

1. Introduction

Species with atmospheric lifetimes of months or less are considered very short-lived (VSL) substances since their chemical lifetimes are similar to tropospheric transport time scales. Ozone depletion in the upper troposphere can occur when the degradation of VSL source gases produces enough inorganic halogen. While the emphasis has been on inorganic chlorine, other inorganic halogens (i.e., bromine and iodine) have the capacity of depleting stratospheric ozone.[1–3] Typically, the observed concentrations of VSL halogen source gases proceed from natural sources and range in a few ppt for Br and I.[3,4] Brominated compounds, when transported and photolyzed in the stratosphere, can produce Br atoms that participate in catalytic ozone destruction 40−50 times more effectively than Cl atoms.[5–9] It has not been easy to estimate the impact of VSL halogen source gases on stratospheric ozone, mostly because of physical and dynamical processes affecting the transport of the halogen to the stratosphere.[3] The degradation pathways of their intermediate degradation products play an important role as well. Usually, the expected degradation products are readily converted to inorganic halogen.

There has been an increasing interest in replacing chlorofluorocarbons (CFCs) and several other halocarbons as part of the agreements of the Montreal Protocol on Substances that Deplete the Ozone Layer.[10,11] A number of the compounds proposed as replacements for the substances controlled under the Montreal Protocol have short atmospheric lifetimes. An important example is bromopropane. Bromopropane ($BrCH_2CH_2CH_3$), also known as *n*-propyl bromide (*n*-PB) and 1-bromopropane (1-BP), has been considered as a replacement for CFCs used as the active component of industrial cleaning solvents,[11–14] more specifically HCFC-141b.[15] It is also a VSL substance known to release Br atoms 2−3 times more effectively than some CFCs would release Cl atoms in the lower stratosphere.[13] For many compounds, reaction with the hydroxyl radical (OH) is considered the most effective "cleaning method" of the atmosphere from natural and anthropogenic gases that could create a buildup of atmospheric gases contributing to the greenhouse effect.[3,16,17] Modeling[11,18–20] and kinetic[12–15,21,22] studies have demonstrated that the primary atmospheric sink of *n*-PB is its reaction with OH, with an atmospheric lifetime of 10−16 days. One of the challenges of modeling the atmospheric impact of compounds such as bromopropane is determining its ability to affect concentrations of stratospheric ozone. In particular, one needs to determine what amount of bromopropane, and its reaction products, reaches the stratosphere where the Br released can react to destroy ozone. The amount of Br that would be available to affect stratospheric ozone greatly depends on transport and chemical removal processes in the troposphere. Research on VSL species, such as bromopropane, has demonstrated the dependency of the atmospheric lifetime on the geographic distribution of surface emissions of the scavenger.[3,13,14,19,20] It has been previously determined that photolysis and an estimated ocean sink have an insignificant effect on the residence time of bromopropane in the atmosphere.[11,22]

Being a less photolabile compound, the degradation mechanism of bromopropane is initiated via its reaction with OH, as previously discussed.[3,11–15,18–22] For purposes of clarity in this article, the halogenated carbon will be called the α carbon, the one next to it the β carbon, and the carbon on the end of the chain the γ carbon. There are three possible pathways that the reaction can undergo, α, β, and γ H-abstraction, which will lead to the formation of different degradation products. These possible pathways and their particular radicals can be observed in reactions 1a, 1b, and 1c.

$$BrCH_2CH_2CH_3 + OH \xrightarrow{\alpha} BrCHCH_2CH_3 + H_2O \quad (1a)$$

$$\xrightarrow{\beta} BrCH_2CHCH_3 + H_2O \quad (1b)$$

$$\xrightarrow{\gamma} BrCH_2CH_2CH_2 + H_2O \quad (1c)$$

Gilles and co-workers,[12] using pulsed laser photolysis followed by laser-induced fluorescence and G3 ab initio calculations, determined the branching ratio of the reaction at room temperature to be a 56, 32, and 12% yield for the β, α, and γ H-abstraction, respectively. The radical species produced are

* To whom correspondence should be addressed.

10.1021/jp8034506 CCC: $40.75
Published on Web 07/31/2008

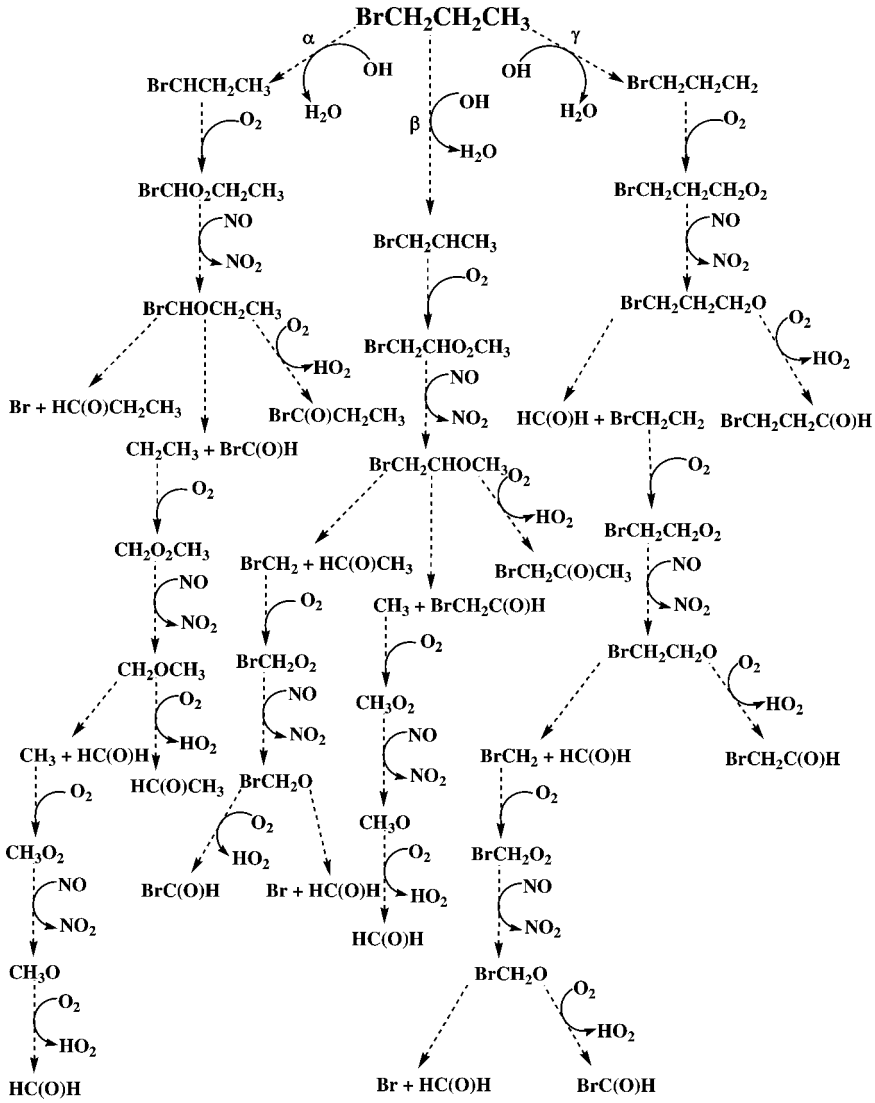

Figure 1. Atmospheric degradation pathways of bromopropane.

readily converted to more stable substances via reaction with O_2. Once the organic peroxy radicals (RO_2) are formed, the degradation continues via reaction with nitric oxide (NO), where oxygen is abstracted to form NO_2 and the alkoxy radical (RO). This alkoxy radical will either undergo unimolecular decomposition or will further react with O_2 to continue the atmospheric degradation of bromopropane through the degradation of its intermediate degradation products. The yield of the degradation products will depend on the atmospheric conditions and on the concentration of the scavengers (i.e., OH, O_2, and NO). Both bromoacetone[3,12] and propanal[12] have been observed in laboratory experiments as products. It is known that all of the degradation products of bromopropane that are not removed by dry or wet deposition release Br atoms to the atmosphere.[20] The Br released in the troposphere and transported to the stratosphere is known to be responsible for the stratospheric effect of bromopropane.

The atmospheric degradation of bromopropane has been previously studied by Wuebbles and co-workers[20] by means of two-dimensional and three-dimensional chemical-transport models in order to determine more accurate ozone depletion potential (ODP) and atmospheric lifetime values. The most significant finding from the modeling studies of Wuebbles and co-workers[20] is that the degradation of bromopropane produces a significant quantity of bromoacetone, which increases the amount of Br transported to the stratosphere due to bromopropane. None of the experimental or modeling studies have ascertained whether the degradation of bromopropane might produce other bromine reservoir species that could carry Br into the stratosphere. The modeling studies of Wuebbles and co-workers[20] also suggest that a complete understanding of the degradation process is essential to accessing the atmospheric effects and ODP of short-lived atmospheric species such as bromopropane. In this article, we present a complete degradation mechanism for the atmospheric oxidation of bromopropane in order to account for the possible ways of obtaining other brominated species not yet accounted for in the boundary experiments or modeling studies.

2. Computational Methods

All calculations were performed with the Gaussian 03 suite of programs.[23] The geometries of the molecules under study were fully optimized and their frequencies obtained. The optimization and subsequent frequency calculations were performed with the second-order Møller−Plesset (MP2) perturbation method. All of the optimizations were done with all electrons unfrozen in the MP2 optimization. The frequency calculations provided all of the thermochemical data and vibrational frequencies of the species involved in the mechanism under study as well as the transition states. Zero-point energy

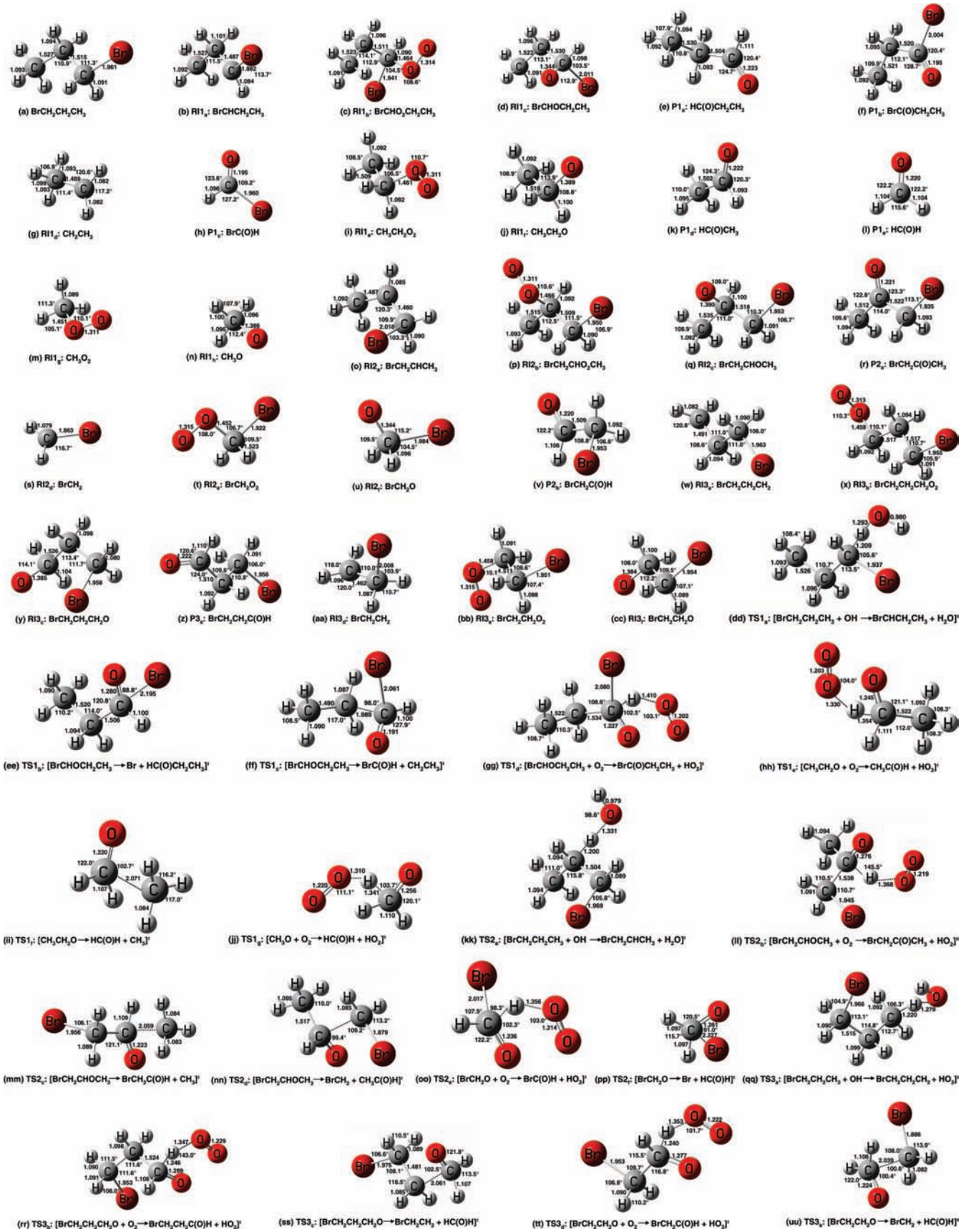

Figure 2. Structures of the atmospheric degradation of bromopropane.

(ZPE) corrections were added to the energetics. The optimized geometries obtained at the MP2 level were used in a series of single-point energy calculations involving the following level of theory and basis set combinations: CCSD(T)/6-311G(2d,2p) and CCSD(T)/6-311++G(2df,2p). The calculated energies were corrected by using the ZPE obtained at the MP2 level in order to obtain the total energies of the various species. These total energies were then used to determine the zero-point-energy-

TABLE 1: Enthalpies of Reaction at 0 K ($\Delta H_{rxn,0\,K}$) in kcal/mol for the Reactions Involved in the Atmospheric Degradation of Bromopropane

reactions	MP2/6-31G(d)[a]	CCSD(T)/6-311G(2d,2p)[a]	CCSD(T)/6-311++G(2df,2p)[a]
	Pathway #1		
$BrCH_2CH_2CH_3 + OH \rightarrow BrCHCH_2CH_3 + H_2O$	−13.2	−16.3	−18.9
$BrCHCH_2CH_3 + O_2 \rightarrow BrCHO_2CH_2CH_3$	−22.5	−27.0	−41.6
$BrCHO_2CH_2CH_3 + NO \rightarrow BrCHOCH_2CH_3 + NO_2$	−24.7	−14.5	−4.3
$BrCHOCH_2CH_3 \rightarrow Br + HC(O)CH_2CH_3$	−10.5	−10.5	−9.8
$BrCHOCH_2CH_3 \rightarrow BrC(O)H + CH_2CH_3$	2.6	3.5	3.7
$BrCHOCH_2CH_3 + O_2 \rightarrow BrC(O)CH_2CH_3 + HO_2$	−32.3	−38.4	−40.0
$CH_2CH_3 + O_2 \rightarrow CH_3CH_2O_2$	−22.5	−29.2	−31.9
$CH_3CH_2O_2 + NO \rightarrow CH_3CH_2O + NO_2$	−21.0	−10.2	−12.2
$CH_3CH_2O + O_2 \rightarrow CH_3C(O)H + HO_2$	−23.9	−30.7	−32.9
$CH_3CH_2O \rightarrow HC(O)H + CH_3$	6.6	8.4	8.7
$CH_3 + O_2 \rightarrow CH_3O_2$	−18.8	−25.8	−28.6
$CH_3O_2 + NO \rightarrow CH_3O + NO_2$	−21.4	−10.5	−12.7
$CH_3O + O_2 \rightarrow HC(O)H + HO_2$	−18.7	−26.1	−27.9
	Pathway #2		
$BrCH_2CH_2CH_3 + OH \rightarrow BrCH_2CHCH_3 + H_2O$	−16.5	−18.8	−21.6
$BrCH_2CHCH_3 + O_2 \rightarrow BrCH_2CHO_2CH_3$	−20.8	−26.9	−29.2
$BrCH_2CHO_2CH_3 + NO \rightarrow BrCH_2CHOCH_3 + NO_2$	−20.0	−9.5	−11.6
$BrCH_2CHOCH_3 + O_2 \rightarrow BrCH_2C(O)CH_3 + HO_2$	−25.4	−31.9	−34.2
$BrCH_2CHOCH_3 \rightarrow BrCH_2C(O)H + CH_3$	3.8	6.0	5.8
$BrCH_2CHOCH_3 \rightarrow BrCH_2 + HC(O)CH_3$	3.9	4.0	3.5
$BrCH_2 + O_2 \rightarrow BrCH_2O_2$	−17.8	−23.5	−26.2
$BrCH_2O_2 + NO \rightarrow BrCH_2O + NO_2$	−26.9	−16.1	−17.9
$BrCH_2O + O_2 \rightarrow BrC(O)H + HO_2$	−27.2	−33.6	−35.2
$BrCH_2O \rightarrow Br + HC(O)H$	−10.1	−9.1	−7.8
	Pathway #3		
$BrCH_2CH_2CH_3 + OH \rightarrow BrCH_2CH_2CH_2 + H_2O$	−11.6	−13.8	−16.5
$BrCH_2CH_2CH_2 + O_2 \rightarrow BrCH_2CH_2CH_2O_2$	−21.3	−28.4	−30.7
$BrCH_2CH_2CH_2O_2 + NO \rightarrow BrCH_2CH_2CH_2O + NO_2$	−20.9	−9.2	−11.6
$BrCH_2CH_2CH_2O + O_2 \rightarrow BrCH_2CH_2C(O)H + HO_2$	−23.0	−30.2	−32.5
$BrCH_2CH_2CH_2O \rightarrow BrCH_2CH_2 + HC(O)H$	5.1	5.6	5.6
$BrCH_2CH_2 + O_2 \rightarrow BrCH_2CH_2O_2$	−20.5	−26.6	−28.9
$BrCH_2CH_2O_2 + NO \rightarrow BrCH_2CH_2O + NO_2$	−22.0	−11.1	−13.4
$BrCH_2CH_2O + O_2 \rightarrow BrCH_2C(O)H + HO_2$	−21.2	−28.0	−30.3
$BrCH_2CH_2O \rightarrow BrCH_2 + HC(O)H$	9.4	9.2	9.1

[a] Corrected with ZPE.

corrected energy barrier (EB_a), as well as the enthalpies of reaction at 0 K ($\Delta H_{rxn,0\,K}$) involved in the mechanism under study.

3. Results and Discussions

3.1. Reaction Pathways in the Atmospheric Degradation of Bromopropane. ***3.1.1. Structures of the Species Involved in the Atmospheric Degradation of Bromopropane.*** As shown in Figure 2a, bromopropane is composed of three different hydrogen environments. The hydrogens in the β and γ carbons have bond lengths of 1.094 and 1.093 Å, whereas the ones in the α carbon have bond lengths of 1.091 Å. The C−Br bond has a length of 1.961 Å.

In the first step of the pathway, the reaction with OH proceeds by the H-abstraction from the α carbon, generating a radical on the halogenated carbon, $BrCHCH_2CH_3$ (Figure 2b). This abstraction causes changes in the structure of the parent molecule when compared to the radical formed. The C−Br bond length decreases to 1.882 Å, and the one hydrogen on the halogenated carbon has a bond length of 1.084 Å. Also, the $C_\alpha-C_\beta$ bond decreases from 1.515 to 1.487 Å as the radical is formed. Once the radical is formed, it readily reacts with O_2 to form the corresponding peroxy radical, $BrCHO_2CH_2CH_3$ (Figure 2c), which in turn reacts with NO to form $BrCHOCH_2CH_3$ (Figure 2d). Currently, the C−Br bond length is 2.011 Å, and the C−O bond has a length of 1.344 Å. At this point, the pathway is divided into three separate pathways. One pathway is the unimolecular decomposition of $BrCHOCH_2CH_3$ to form Br plus $HC(O)CH_2CH_3$. As illustrated in Figure 2e, the final product $HC(O)CH_2CH_3$ has a CO bond of 1.223 Å and a CCO angle of 124.7°. On the other hand, it is also a possibility that the alkoxy radical will react with O_2 to form HO_2 and $BrC(O)CH_2CH_3$ (Figure 2f). In this case, the CO bond is shortened to 1.195 Å, and the CCO angle is 128.7°. Also, the C−Br length is 2.004 Å, and the BrCO angle is 120.4°. Alternatively, a unimolecular decomposition to form CH_2CH_3 (Figure 2g) and BrC(O)H (Figure 2h) can occur. As observed in Figure 2h, this brominated aldehyde has a C−Br bond of 1.960 Å and a CO bond of 1.195 Å. When an O_2 molecule attaches to the vacant site on the CH_2CH_3 and forms $CH_3CH_2O_2$ (Figure 2i), the latter undergoes a reduction as it reacts with NO to form the alkoxy radical CH_3CH_2O (Figure 2j), which will be oxidized by O_2 to yield $HC(O)CH_3$ (Figure 2k). This aldehyde has a CO bond length of 1.222 Å and the CCO angle of 124.3°. A unimolecular decomposition of the alkoxy radical can produce CH_3 and HC(O)H (Figure 2l). Formaldehyde is a symmetric molecule with a CO bond length of 1.220 Å and HCO angles of 122.2°. The CH_3 radical formed will repeat the oxidation and reduction cycles until it forms CH_3O (Figure 2n), which will be oxidized by O_2 to give another formaldehyde molecule.

Another possible site for the hydrogen to be abstracted by OH is from the carbon β to the bromine. This β abstraction

TABLE 2: Zero-Point-Energy-Corrected Energy Barrier (EB_a) in kcal/mol for the Transition States Involved in the Atmospheric Degradation of Bromopropane

transition states	MP2/6-31G(d)[a]	CCSD(T)/6-311G(2d,2p)[a]	CCSD(T)/6-311++G(2df,2p)[a]
	Pathway #1		
$[BrCH_2CH_2CH_3 + OH \rightarrow BrCHCH_2CH_3 + H_2O]^{\ddagger}$	6.9	1.8	0.9
$[BrCHOCH_2CH_3 + O_2 \rightarrow BrC(O)CH_2CH_3 + HO_2]^{\ddagger}$	3.5	2.1	1.3
$[BrCHOCH_2CH_3 \rightarrow Br + HC(O)CH_2CH_3]^{\ddagger}$	4.8	0.0	−0.2
$[BrCHOCH_2CH_3 \rightarrow BrC(O)H + CH_2CH_3]^{\ddagger}$	14.1	10.6	10.3
$[CH_3CH_2O + O_2 \rightarrow CH_3C(O)H + HO_2]^{\ddagger}$	33.1	10.0	4.1
$[CH_3CH_2O \rightarrow HC(O)H + CH_3]^{\ddagger}$	25.0	18.3	17.9
$[CH_3O + O_2 \rightarrow HC(O)H + HO_2]^{\ddagger}$	40.0	16.1	14.3
	Pathway #2		
$[BrCH_2CH_2CH_3 + OH \rightarrow BrCH_2CHCH_3 + H_2O]^{\ddagger}$	6.2	1.4	0.2
$[BrCH_2CHOCH_3 + O_2 \rightarrow BrCH_2C(O)CH_3 + HO_2]^{\ddagger}$	8.3	5.6	4.5
$[BrCH_2CHOCH_3 \rightarrow BrCH_2C(O)H + CH_3]^{\ddagger}$	23.0	16.6	16.0
$[BrCH_2CHOCH_3 \rightarrow BrCH_2 + HC(O)CH_3]^{\ddagger}$	23.5	16.5	15.3
$[BrCH_2O + O_2 \rightarrow BrC(O)H + HO_2]^{\ddagger}$	7.0	3.7	2.8
$[BrCH_2O \rightarrow Br + HC(O)H]^{\ddagger}$	8.8	2.4	2.2
	Pathway #3		
$[BrCH_2CH_2CH_3 + OH \rightarrow BrCH_2CH_2CH_2 + H_2O]^{\ddagger}$	7.8	3.8	2.7
$[BrCH_2CH_2CH_2O + O_2 \rightarrow BrCH_2CH_2C(O)H + HO_2]^{\ddagger}$	8.3	5.8	4.8
$[BrCH_2CH_2CH_2O \rightarrow BrCH_2CH_2 + HC(O)H]^{\ddagger}$	20.7	13.6	13.2
$[BrCH_2CH_2O \rightarrow BrCH_2 + HC(O)H]^{\ddagger}$	25.9	18.4	17.5
$[BrCH_2CH_2O + O_2 \rightarrow BrCH_2C(O)H + HO_2]^{\ddagger}$	9.8	6.5	5.3

[a] Corrected with ZPE.

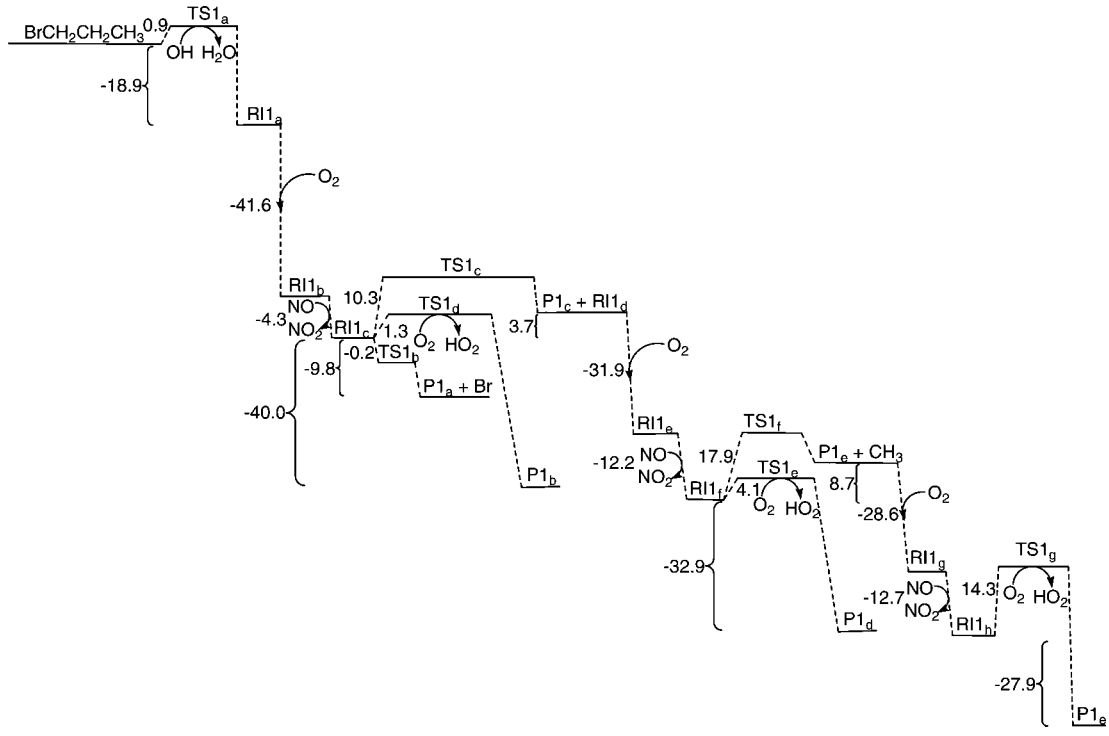

Figure 3. Potential energy surface for the hydrogen abstraction from the α carbon during the atmospheric degradation of bromopropane using the CCSD(T)/6-311++G(2df,2p)//MP2/6-31G(d) level of theory.

will lead to $BrCH_2CHCH_3$. As it is illustrated in Figure 2o, the $C_\alpha-C_\beta$ has changed from the parent molecule from 1.515 to 1.460 Å. As well, the $C_\beta-C_\gamma$ has changed from the parent molecule from 1.527 to 1.487 Å. Also, the hydrogen in the β carbon decreased its length to 1.085 Å. This radical will be oxidized by O_2, forming $BrCH_2CHO_2CH_3$ (Figure 2p), which will be reduced by NO to form $BrCH_2CHOCH_3$ (Figure 2q). At this point, the β C−H bond increases to 1.100 Å, and the new CO bond has a length of 1.390 Å. The HCO angle is 109.0°, while the CCC angle is 111.0°. Similarly to the first pathway, this alkoxy radical will undergo several ways of unimolecular decomposition or oxidations. Its oxidation will give rise to HO_2 and $BrCH_2C(O)CH_3$ (Figure 2r). This oxidation product has an increased CCC angle of 114.0° and a shortened CO bond of 1.221 Å. One of the possible unimolecular decompositions available to $BrCH_2CHOCH_3$ will produce $BrCH_2C(O)H$ and CH_3, which will end up producing a formaldehyde molecule, as explained previously in Pathway 1. As illustrated in Figure 2v, $BrCH_2C(O)H$ is an aldehyde that has a CO bond length of 1.220 Å and a CCO angle of 122.5°. On the other hand, an will produce $HC(O)CH_3$ and $BrCH_2$ (Figure 2s). As observed in Figure 1, the brominated radical will be oxidized by molecular oxygen to form $BrCH_2O_2$ (Figure 2t), which will be reduced by NO producing $BrCH_2O$ (Figure 2u). This alkoxy radical

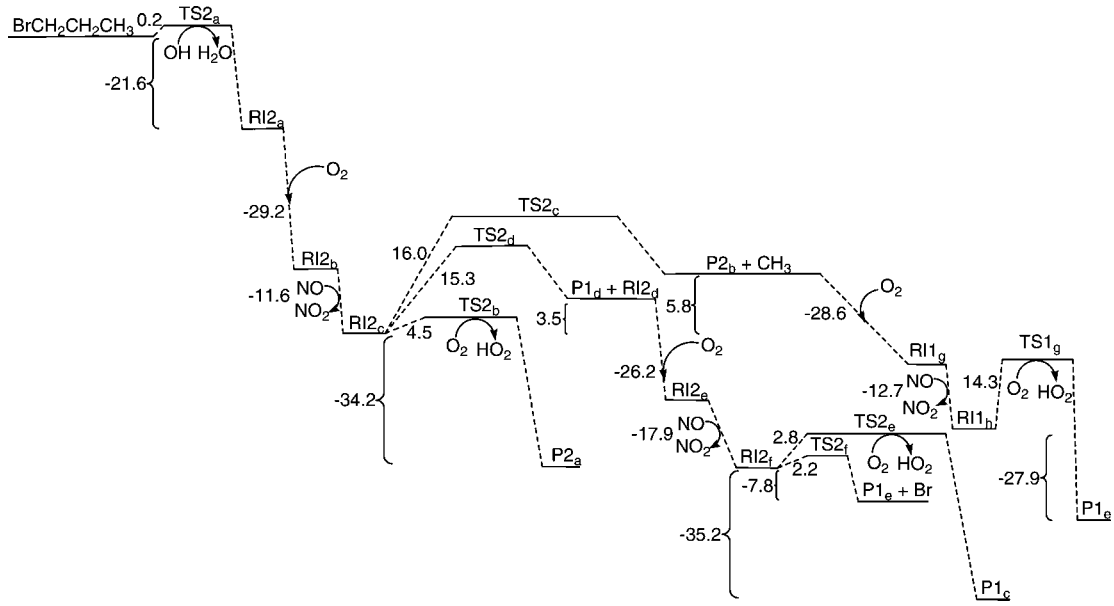

Figure 4. Potential energy surface for the hydrogen abstraction from the β carbon during the atmospheric degradation of bromopropane using the CSD(T)/6-311++G(2df,2p)//MP2/6-31G(d) level of theory.

would either be oxidized, forming BrC(O)H, or will form Br and formaldehyde.

The abstraction of a hydrogen on the γ site will lead to $BrCH_2CH_2CH_2$ (Figure 2w). This radical has a $C_\beta-C_\gamma$ bond length of 1.491 Å and CH bond lengths at the attacked carbon of 1.082 Å. As in the previous pathways, this radical will react with O_2 to form the peroxy radical, $BrCH_2CH_2CH_2O_2$ (Figure 2x). The peroxy radical is reduced to an alkoxy radical, $BrCH_2CH_2CH_2O$ (Figure 2y), via reaction with NO. This alkoxy radical can undergo an oxidation that will produce $BrCH_2CH_2C(O)H$ and HO_2. As observed in Figure 2z, $BrCH_2CH_2C(O)H$ has a CO bond length of 1.222 Å and a HCO angle of 120.6°. On the other hand, a unimolecular decomposition will produce formaldehyde and $BrCH_2CH_2$ (Figure 2aa). A cycle of oxidation and reduction by O_2 and NO, respectively, will lead to $BrCH_2CH_2O$. As observed in Figure 2cc, $BrCH_2CH_2O$ has a CO bond of 1.384 Å and a HCO angle of 108.0°. Also, the CC bond has a length of 1.519 Å. The newly formed radical will either undergo an oxidation to form $BrCH_2C(O)H$ or a unimolecular decomposition to form formaldehyde and $BrCH_2$. The $BrCH_2$ radical will produce Br, formaldehyde, and BrC(O)H, as previously discussed in Pathway 2.

3.1.2. Energetics of the Species Involved in the Atmospheric Degradation of Bromopropane. The overall reaction mechanism is shown in Figure 1. Tables 1 and 2 list all the enthalpies of reaction at 0 K and the zero-point-energy-corrected reaction energy barrier (EB_a) calculated for the atmospheric degradation mechanism of bromopropane.

A schematic containing the calculated enthalpies of reaction and energy barriers for Pathway 1 can be observed in the energetics diagram, Figure 3. Pathway 1 is the oxidation process that results from the hydrogen abstraction from the α carbon. The first step on this pathway is the reaction of bromopropane with the OH scavenger. The enthalpy of reaction is predicted to be −18.9 kcal/mol at the CCSD(T)/6-311++G(2df,2p)//MP2/6-31G(d) level of theory. The barrier height for the hydrogen abstraction is predicted to be 0.9 kcal/mol at the same level of theory. The transition state is a first-order saddle point with an imaginary frequency at 2242 cm^{-1}. Tunneling will be important for this reaction. The formed radical, $BrCHCH_2CH_3$, will undergo a reaction with O_2 with a formation energy cost of −41.6 kcal/mol. Subsequently, the formed organic peroxy radical will react with NO, breaking the OO bond to form NO_2. This bond-breaking and bond-forming process will have a $\Delta H_{rxn,\,0\,K}$ of −4.3 kcal/mol.

The alkoxy radical formed, $BrCHOCH_2CH_3$, may participate in the following reaction channels:

$$BrCHOCH_2CH_3 \rightarrow Br + HC(O)CH_2CH_3 \quad (2)$$

$$BrCHOCH_2CH_3 \rightarrow BrC(O)H + CH_2CH_3 \quad (3)$$

$$BrCHOCH_2CH_3 + O_2 \rightarrow BrC(O)CH_2CH_3 + HO_2 \quad (4)$$

Reaction 2 represents a unimolecular decomposition of the radical in which the C−Br bond is broken and a C═O bond is formed. This process has an enthalpy of reaction at 0 K and barrier heights of −9.8 and −0.2 kcal/mol, respectively. Reaction 3 is another unimolecular decomposition in which the CC bond is broken and a C═O bond is formed with an energy barrier of 10.3 kcal/mol. The reaction is only to some extent endothermic, with a reaction enthalpy of 3.7 kcal/mol. On the other hand, reaction 4 represents a stabilization of the alkoxy radical via a reaction with O_2. In this process, a hydrogen abstraction occurs with an energy barrier and an enthalpy of reaction at 0 K of 1.3 and −40.0 kcal/mol, respectively. Through vibrational frequency analysis, the first-order saddle points for reactions 2, 3, and 4 were found to be at 591, 501, and 871 cm^{-1}, respectively.

Reaction 3 produces a CH_2CH_3 radical that will stabilize reacting with O_2, having a $\Delta H_{rxn,\,0\,K}$ of −31.9 kcal/mol. The newly formed organic peroxy radical, $CH_3CH_2O_2$, will react with the NO scavenger where the OO bond will be broken and another NO bond formed. This will have a formation cost of −12.2 kcal/mol. The formed CH_3CH_2O can undergo two different reaction channels

$$CH_3CH_2O + O_2 \rightarrow CH_3C(O)H + HO_2 \quad (5)$$

$$CH_3CH_2O \rightarrow HC(O)H + CH_3 \quad (6)$$

Reaction 5 involves a hydrogen abstraction via the reaction of the alkoxy radical with molecular oxygen. The enthalpy of reaction for this is −32.9 kcal/mol. The calculated energy barrier for reaction 5 is 4.1 kcal/mol. The unimolecular decomposition

where the CC bond is broken and a C═O bond is formed is represented in reaction 6. The barrier height for the CC breakage is predicted to be 17.9 kcal/mol, and the $\Delta H_{rxn,0\,K}$ is 8.7 kcal/mol. The obtained transition states were characterized by one imaginary frequency at 3234 and 687 cm^{-1} for reactions 5 and 6, respectively. The CH_3 radical produced in reaction 6 reacts with O_2 under a −28.6 kcal/mol enthalpy of reaction at 0 K. The organic peroxy radical formed will react with NO, and the subsequent alkoxy radical will react with O_2 for formation costs of −12.7 and −27.9 kcal/mol, respectively. In this last step of the pathway, the formation of HC(O)H and HO_2 involves a barrier height of 14.3 kcal/mol. The first-order saddle point was found to be at 3744 cm^{-1}.

A schematic containing the calculated energetics for Pathway 2 can be observed in Figure 4. Pathway 2 is the oxidation process that results from the hydrogen abstraction from the β carbon. After performing the calculations for all 3 pathways under discussion, abstracting the hydrogen from the β carbon is considered the most kinetically favorable pathway. This is because it has to overcome the smallest energy barrier of all three pathways, 0.2 kcal/mol. The first-order saddle point was indicated by one negative frequency at 1858 cm^{-1}. This reaction has a $\Delta H_{rxn,0\,K}$ of −21.6 kcal/mol. Following the hydrogen abstraction, the radical formed in the first step of the pathway will react with O_2 to form the corresponding organic peroxy radical. Therefore, when $BrCH_2CHCH_3$ reacts with O_2, it creates an organic peroxy radical with a new CO bond; this step has an enthalpy of reaction at 0 K of −29.2 kcal/mol. Subsequently, $BrCH_2CHO_2CH_3$ will react with NO to form the corresponding alkoxy radical and NO_2 by breaking a CO bond. This bond-breaking and bond-formation step has a formation energy cost of −11.6 kcal/mol.

The alkoxy radical $BrCH_2CHOCH_3$ can be removed by the following reaction channels:

$$BrCH_2CHOCH_3 + O_2 \rightarrow BrCH_2C(O)CH_3 + HO_2 \quad (7)$$

$$BrCH_2CHOCH_3 \rightarrow BrCH_2C(O)H + CH_3 \quad (8)$$

$$BrCH_2CHOCH_3 \rightarrow BrCH_2 + HC(O)CH_3 \quad (9)$$

Reaction 7 represents the removal of the radical by reaction with molecular oxygen. The channel represented by reaction 7 is kinetically favorable since the energy barrier that it has to overcome is only 4.5 kcal/mol, and this means that the most favorable end products for Pathway 2 are $BrCH_2C(O)CH_3$ and HO_2. The enthalpy of reaction at 0 K for such a reaction is −34.2 kcal/mol. The unimolecular decomposition represented in reaction 8 is endothermic by 5.8 kcal/mol, with a barrier height of 16.0 kcal/mol. The transition states for reactions 7 and 8 were attributed one negative frequency at 1783 and 745 cm^{-1}, respectively. The CH_3 formed as part of reaction 8 will undergo the degradation mechanism explained in Pathway 1. Reaction 9 represents a CC bond fission reaction. It has an energy barrier of 15.3 kcal/mol, whereas the enthalpy of reaction at 0 K is 3.5 kcal/mol. It is a first-order saddle point with an imaginary frequency of 841 cm^{-1}. Now reactions 8 and 9 are very dependent on the internal energy and pressure because collsions will remove the excess energy. If the unimolecular rate is fast, then the $BrCH_2CHOCH_3$ radical may decompose before collisions can occur with molecular oxygen, reaction 7. In that case, reaction 9 would be kinetically favored. Reaction 7 will tend to be favored at higher pressures, while reactions 8 and 9 will tend to be favored at lower pressures (hence, higher altitudes).The $BrCH_2$ radical formed from reraction 9 will react with O_2, and this reaction is exothermic by 26.2 kcal/mol. The newly formed organic peroxy radical, $BrCH_2O_2$, will react with the NO scavenger where the OO bond will be broken and another NO bond formed. This will have a $\Delta H_{rxn,0\,K}$ of −17.9 kcal/mol. The $BrCH_2O$ alkoxy radical can undergo two separate reactions. On the one hand, the radical can easily react with O_2 to form BrC(O)H and HO_2. This reaction will have a barrier height and an enthalpy of reaction at 0 K of 2.8 and −35.2 kcal/mol, respectively. On the other hand, the dissociation of the alkoxy radical has an energy barrier of 2.2 kcal/mol. At the same time, the $\Delta H_{rxn,0\,K}$ reaches −7.8 kcal/mol. Vibrational

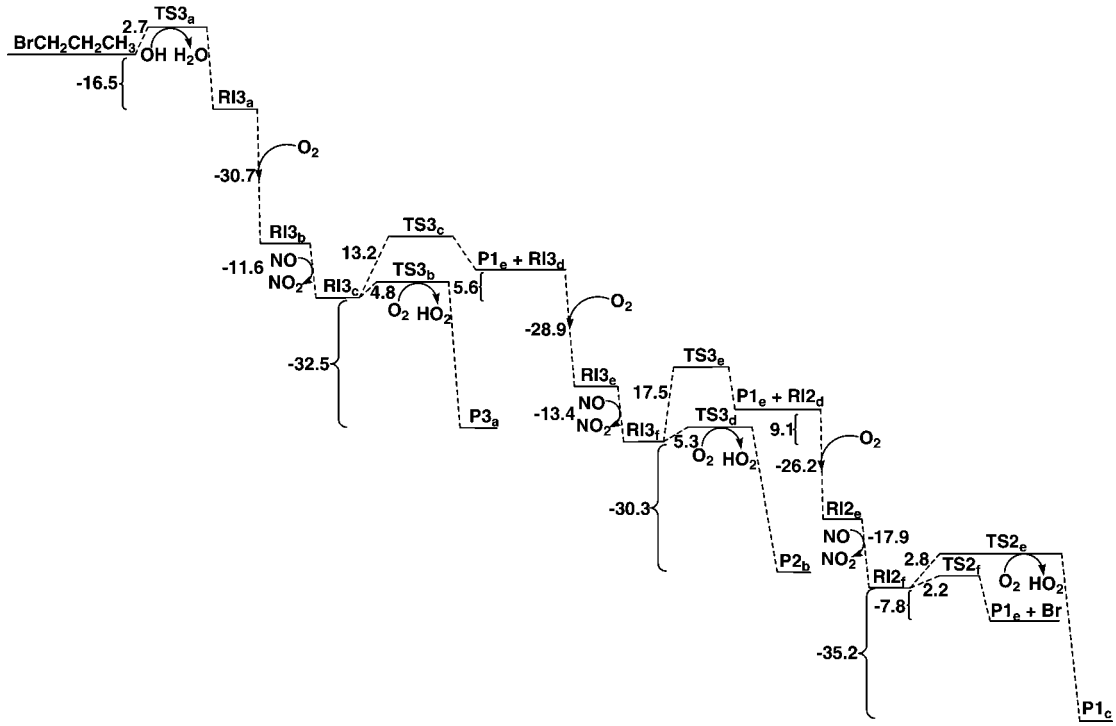

Figure 5. Potential energy surface for the hydrogen abstraction from the γ carbon during the atmospheric degradation of bromopropane using the CCSD(T)/6-311++G(2df,2p)//MP2/6-31G(d) level of theory.

frequency analysis identified the first-order saddle points to be 522 and 623 cm^{-1} for the $BrCH_2O$ reaction with O_2 and the unimolecular decomposition, respectively.

Figure 5 is a schematic that contains the calculated energetics for Pathway 3. The abstraction of the γ hydrogen has been observed as the least kinetically favorable pathway for bromopropane to undergo. Pathway 3 is the oxidation process that results from the hydrogen abstraction from the γ carbon. This reaction will have a barrier height and an enthalpy of reaction at 0 K of 2.7 and −16.5 kcal/mol, respectively. The imaginary frequency attributed to the first-order saddle point was found to be at 2254 cm^{-1}. The formed $BrCH_2CH_2CH_2$ reacts with O_2 with an enthalpy of reaction at 0 K of −30.7 kcal/mol. The organic peroxy radical reacts with NO in order to form NO_2, breaking the OO bond. This reaction has a $\Delta H_{rxn,\,0\,K}$ of −11.6 kcal/mol. The alkoxy radical $BrCH_2CH_2CH_2O$, formed as a result of the NO reduction of the organic peroxy radical, can undergo two different reaction channels

$$BrCH_2CH_2CH_2O + O_2 \rightarrow BrCH_2CH_2C(O)H + HO_2 \quad (10)$$

$$BrCH_2CH_2CH_2O \rightarrow BrCH_2CH_2 + HC(O)H \quad (11)$$

The hydrogen abstraction represented in reaction 10 is obtained after an energy barrier of 4.8 kcal/mol. The enthalpy of reaction at 0 K for this reaction is −32.5 kcal/mol. On the other hand, products from the decomposition of $BrCH_2CH_2CH_2O$ in reaction 11 are obtained after overcoming a barrier height of 13.2 kcal/mol. The reaction is, to some extent, endothermic, with a reaction enthalpy of 5.6 kcal/mol. The first-order saddle points for reactions 10 and 11 were located with imaginary frequencies values of 1894 and 635 cm^{-1}, respectively. The $BrCH_2CH_2$ radical underwent a reaction with O_2 in order to form $BrCH_2CH_2O_2$, which had a formation cost of −28.9 kcal/mol. The organic peroxy radical reacted with NO under a $\Delta H_{rxn,\,0\,K}$ of −13.4 kcal/mol. The resulting alkoxy radical can either undergo a reaction with O_2 or a unimolecular decomposition. The reaction with O_2 has to overcome an energy barrier of 5.3 kcal/mol and an enthalpy of reaction at 0 K of −30.3 kcal/mol. On the other hand, the barrier for the unimolecular dissociation is 17.5 kcal/mol with a $\Delta H_{rxn,\,0\,K}$ of 9.1 kcal/mol. The resulting $BrCH_2$ radical will undergo the degradation mechanism explained in Pathway 2. Transition-state structures were characterized by one negative frequency with values of 1856 and 736 cm^{-1} for the $BrCH_2CH_2O$ reaction with O_2 and the unimolecular decomposition, respectively.

3.2. Atmospheric Implications. The atmospheric oxidation mechanism of bromopropane has been thoroughly assessed in this article. Previously, Gilles and co-workers[12,24] reported the product branching ratios for the reaction of bromopropane with the OH scavenger. Using pulsed laser photolysis followed by laser-induced fluorescence, the group determined that the α, β, and γ abstractions have a 32, 56, and 12% yield at room temperature, respectively. These findings are consistent with the predictions obtained by the present ab initio calculations results. Our studies revealed that the hydrogen abstraction from the β carbon has the lowest energy barrier (0.2 kcal/mol) of all of the possible abstractions. Therefore, this would be the most energetically favored pathway for the atmospheric oxidation process. Wuebbles and co-workers[20] proposed a possible mechanism for the reaction among the OH scavenger and bromopropane. In their 2D and 3D chemical-transport model, the group found that the atmospheric degradation of bromopropane produces significant quantities of bromoacetone ($BrCH_2C(O)CH_3$). This assertion is consistent with our findings. Wuebbles and co-workers[20] assumed that bromoacetone would be the more stable reservoir species resulting from the atmospheric oxidation of bromopropane. The present work suggests additional new chemistry and species ($BrC(O)CH_2CH_3$ and $BrCH_2CH_2C(O)H$) not accounted for in the Wuebbles et al. study of 2001. As a result, new atmospheric modeling studies are needed to assess the importance of the chemistry derived from the present work. As explained previously, the production of bromoacetone is obtained through Pathway 2, which results from the hydrogen abstraction at the β carbon. Bromoacetone is produced after the alkoxy radical reacts with molecular oxygen. This reaction is the one with the lowest energy barrier that the radical can undergo. Bromoacetone is formed after overcoming a 4.5 kcal/mol barrier height, while the unimolecular decompositions that the radical can undergo have barrier heights of 15.3 and 16.0 kcal/mol, respectively. The experimental studies of Gilles and co-workers[12,24] also showed bromoacetone as a stable degradation product. Other studies have mentioned bromoacetone, Br, and $BrCH_2CH_2C(O)H$ as major degradation products of bromopropane.[3] This study shows that the $BrCH_2CH_2C(O)H$ is a result of oxidation initiated at the γ carbon site.

By means of this atmospheric oxidation mechanism, the possible products that could result from the degradation of bromopropane are as follows. For the primary abstraction, the possible end products that should be observed are Br, $HC(O)CH_2CH_3$, $BrC(O)CH_2CH_3$, BrC(O)H, $HC(O)CH_3$, and two HC(O)H. The energetically favored β abstraction route can produce the possible end products Br, $BrCH_2C(O)CH_3$, $BrCH_2C(O)H$, $HC(O)CH_3$, BrC(O)H, and HC(O)H. On the other hand, the tertiary γ abstraction produces Br, $BrCH_2CH_2C(O)H$, $BrCH_2C(O)H$, and BrC(O)H. It is extremely important to note that each of the pathways will produce Br. Our survey of the literature shows that little is known experimentally about the species $BrC(O)CH_2CH_3$, $BrCH_2C(O)H$, and $BrCH_2CH_2C(O)H$. These could be new potential bromine reservoir species resulting from bromopropane in its oxidation in the atmosphere not yet accounted for either experimentally or in atmospheric models.

Acknowledgment. The authors gratefully acknowledge the financial support given by the U.S. Department of Energy, Global Change Education Program-Graduate Research Environmental Fellowship to Mónica Martínez-Avilés. Special thanks are due to Professor Jeffrey S. Gaffney at the University of Arkansas at Little Rock for his valuable comments and discussions.

Supporting Information Available: The calculated total energies of the reactants, reactive intermediates, products, and transition states of the atmospheric degradation of bromopropane are given in Table 1S. Vibrational frequencies of the aforementioned species are given in Table 1S. This material is available free of charge via the Internet at http://pubs.acs.org.

References and Notes

(1) Cicerone, R. J. *Rev. Geophys. Space Phys.* **1981**, *19*, 123.

(2) Finlayson-Pitts, B. J.; Pitts, J. N. *Atmospheric Chemistry: Fundamentals and Experimental Techniques*; John Wiley and Sons, Inc.: New York, 1986.

(3) WMO (World Metereological Organization), 2003.

(4) Yung, Y. L.; Pinto, J. P.; Watson, R. T.; Sander, S. P. *J. Atmos. Sci.* **1980**, *37*, 339.

(5) Dixon, D. A.; Jong, W. A. d.; Peterson, K. A.; Francisco, J. S. *J. Phys. Chem. A* **2002**, *106*, 4725.

(6) WMO (World Metereological Organization), 1990.

(7) Daniel, J. S.; Solomon, S.; Portmann, R. W.; Garcia, R. R. *J. Geophys. Res.* **1999**, *104*, 23871.

(8) Kamboures, M. A.; Hansen, J. C.; Francisco, J. S. *Chem. Phys. Lett.* **2002**, *353*, 335.

(9) Anderson, J. G.; Brune, W. H.; Lloyd, S. A.; Toohey, D. W.; Sander, S. P.; Starr, W. L.; Loewenstein, M.; Podolske, J. R. *J. Geophys. Res.* **1989**, *94*, 11480.

(10) Yu, X.; Ichihara, G.; Kitoh, J.; Xie, Z.; Shibata, E.; Kamijima, M.; Asaeda, N.; Takeuchi, Y. *J. Occup. Health* **1998**, *40*, 234.

(11) Wuebbles, D. J.; Jain, A. K.; Patten, K. O.; Connell, P. S. *Atmos. Environ.* **1997**, *32*, 107.

(12) Gilles, M. K.; Burkholder, J. B.; Gierczak, T.; Marshall, P.; Ravishankara, A. R. *J. Phys. Chem. A* **2002**, *106*, 5358.

(13) Nelson, D. D., Jr.; Wormhoudt, J. C.; Zahniser, M. S.; Kolb, C. E.; Ko, M. K. W.; Weisenstein, D. K. *J. Phys. Chem. A* **1997**, *101*, 4987.

(14) Kozlov, S. N.; Orkin, V. L.; Huie, R. E.; Kurylo, M. J. *J. Phys. Chem. A* **2003**, *107*, 1333.

(15) Herndon, S. C.; Gierczak, T.; Talukdar, R. K.; Ravishankara, A. R. *Phys. Chem. Chem. Phys.* **2001**, *3*, 4529.

(16) Levy, H., II. *Planet. Space Sci.* **1972**, *20*, 919.

(17) Matthews, J.; Sinha, A.; Francisco, J. S. *Proc. Natl. Acad. Sci. U.S.A.* **2005**, *102*, 7449.

(18) Wuebbles, D. J.; Kotamarthi, R.; Patten, K. O. *Atmos. Environ.* **1999**, *33*, 1641.

(19) Bridgeman, C. H.; Pyle, J. A.; Shallcross, D. E. *J. Geophys. Res.* **2000**, *105*, 26493.

(20) Wuebbles, D. J.; Patten, K. O.; Johnson, M. T. *J. Geophys. Res.* **2001**, *106*, 14551.

(21) Donaghy, T.; Shanahan, I.; Hande, M.; Fitzpatrick, S. *Int. J. Chem. Kinet.* **1993**, *25*, 273.

(22) Teton, S.; Boudali, A. E.; Mellouki, A. *J. Chim. Phys.* **1996**, *93*, 274.

(23) Frisch, M. J.; Trucks, G. W.; Schlegel, H. B.; Scuseria, G. E.; Robb, M. A.; Cheeseman, J. R. J. A. ; Montgomery, J.; Vreven, T.; Kudin, K. N.; Burant, J. C.; Millam, J. M.; Iyengar, S. S.; Tomasi, J.; Barone, V.; Mennucci, B.; Cossi, M.; Scalmani, G.; Rega, N.; Petersson, G. A.; Nakatsuji, H.; Hada, M.; Ehara, M.; Toyota, K.; Fukuda, R.; Hasegawa, J.; Ishida, M.; Nakajima, T.; Honda, Y.; Kitao, O.; Nakai, H.; Klene, M.; Li, X.; Knox, J. E.; Hratchian, H. P.; Cross, J. B.; Adamo, C.; Jaramillo, J.; Gomperts, R.; Stratmann, R. E.; Yazyev, O.; Austin, A. J.; Cammi, R.; Pomelli, C.; Ochterski, J. W.; Ayala, P. Y.; Morokuma, K.; Voth, G. A.; Salvador, P.; Dannenberg, J. J.; Zakrzewski, V. G.; Dapprich, S.; Daniels, A. D.; Strain, M. C.; Farkas, O.; Malick, D. K.; Rabuck, A. D.; Raghavachari, K.; Foresman, J. B.; Ortiz, J. V.; Cui, Q.; Baboul, A. G.; Clifford, S.; Cioslowski, J.; Stefanov, B. B.; Liu, G.; Liashenko, A.; Piskorz, P.; Komaromi, I.; Martin, R. L.; Fox, D. J.; Keith, T.; Al-Laham, M. A.; Peng, C. Y.; Nanayakkara, A.; Challacombe, M.; Gill, P. M. W.; Johnson, B.; Chen, W.; Wong, M. W.; Gonzalez, C.; Pople, J. A. *Gaussian 03*, revision B.03; Gaussian, Inc.: Pittsburgh, PA, 2003.

(24) Burkholder, J. B.; Gilles, M. K.; Gierczak, T.; Ravishankara, A. R. *Geophys. Res. Lett.* **2002**, *29*, 1822.

JP8034506